JOC Article

Modeling Mechanisms of Unusual Benzene Imine N6 Adduct Formation in Carcinogenic Reactions of Arylnitrenium Ions with Adenosine

Shi-Fei Qi and Zhong-Zhi Yang*

Chemistry and Chemical Engineering Faculty, Liaoning Normal University, Dalian 116029, People's Republic of China

zzyang@lnnu.edu.cn

Received September 9, 2007

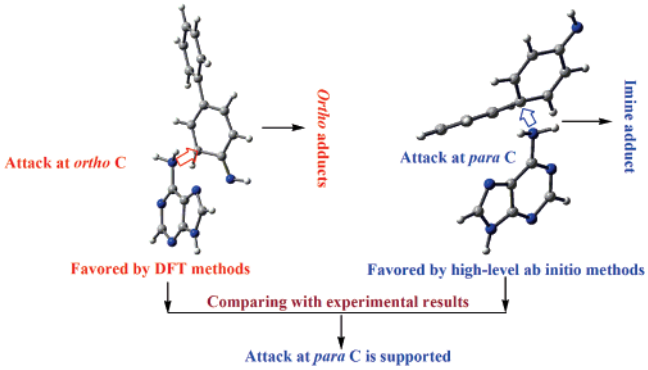

Reaction mechanisms of the unusual benzene imine N6 adduct formation in carcinogenic reactions of arylnitrenium ions with adenosine have been investigated with density functional theory (DFT) and high-level ab initio methods. The DFT calculations indicate that the reaction pathways initiated by attack of adenine at the ortho C site of 4-biphenylylnitrenium ion are favored. However, high-level MP2 and QCISD calculations provide a contrary conclusion, that is the reaction pathways initiated by attack of adenine at the para C site of 4-biphenylylnitrenium ion are more feasible. Comparing with experimental results, the conclusion from high-level ab initio calculations is ultimately supported. The present study makes a theoretical prediction on the final products in the studied reaction, which is in agreement with experimental observations. In addition, this study provides some inspirations to the attacks of arylnitrenium ions at amino group of purines and pyrimidines in similar carcinogenic reactions.

1. Introduction

Nitrenium ions and their related species are involved in many important chemical and biological processes, such as their utility in synthesis,[1] their suspected intermediacy in the synthesis of conducting aniline,[2] and their role in DNA damage caused by enzymatically activated arylamine carcinogens.[3] They are reactive short-lived species that are generally difficult to identify and investigate experimentally.[4] In recent years, however, several techniques have successfully been developed to directly probe these nitrenium ions.[4−9]

(1) (a) Kikugawa, Y.; Kawase, M. *J. Am. Chem. Soc.* **1984**, *106*, 5728. (b) Wardrop, D. J.; Zhang, W. M. *Org. Lett.* **2001**, *3*, 2353.

(2) (a) Ding, Y.; Padias, A. B.; Hall, J. H. K. *J. Polym. Sci. Polym. Chem.* **1999**, *37*, 2569. (b) Wei, Y.; Tang, X.; Sun, Y. *J. Polym. Sci. Polym. Chem.* **1989**, *27*, 2385.

(3) (a) Miller, J. A. *Cancer Res.* **1970**, *30*, 559. (b) Kadlubar, F. F. In *DNA Adducts*: *Identification and Biological Significance*; Hemmink, K. K. A., Shugar, D. E. G., Kadlubar, F. F., Segerback, D., Bartsch, H., Eds.; University Press: Oxford, UK, 1994; p 199. (c) Schut, H. A. J.; Snyderwine, E. G. *Carcinogenesis* **1999**, *20*, 353.

(4) (a)Falvey, D. E. In *Reactive Intermediate Chemistry*; Moss, R. A., Platz, M. S., Maitland Jones, J., Eds.; Wiley-Interscience: Hoboken, NJ, 2004; Vol. 1, p 593. (b) McClelland, R. A. *Tetrahedron* **1996**, *52*, 6823. (c) Novak, M.; Rajagopal, S. *Adv. Phys. Org. Chem.* **2001**, *36*, 167.

(5) (a) Anderson, G. B.; Falvey, D. E. *J. Am. Chem. Soc.* **1993**, *115*, 9870. (b) Robbins, R. J.; Yang, L. L. N.; Anderson, G. B.; Falvey, D. E. *J. Am. Chem. Soc.* **1995**, *117*, 6544. (c) Kung, A. C.; Falvey, D. E. *J. Org. Chem.* **2005**, *70*, 31272.

(6) (a) Davidse, P. A.; Kahley, M. J.; McClelland, R. A.; Novak, M. *J. Am. Chem. Soc.* **1994**, *116*, 4513. (b) McClelland, R. A.; Davidse, P. A.; Hadzialic, G. *J. Am. Chem. Soc.* **1995**, *117*, 4173. (c) McClelland, R. A.; Kahley, M. J.; Davidse, P. A.; Hadzialic, G. *J. Am. Chem. Soc.* **1996**, *118*, 4794.

10.1021/jo701980y CCC: $37.00
Published on Web 11/21/2007

SCHEME 1

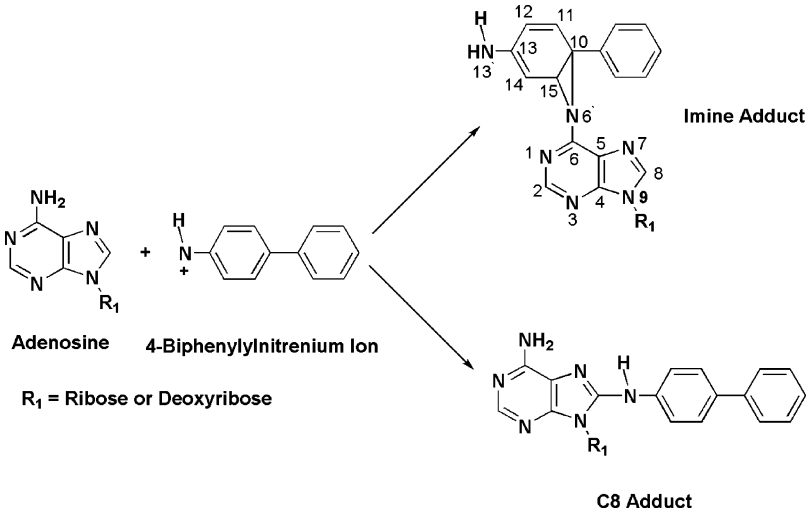

The role of aromatic substituted nitrenium ions in carcinogenic processes is often of concern.[3,7,10] These arylnitrenium ions derive from metabolic oxidation of aromatic amines[11−13] that can be ingested directly, e.g., as cooked food[14] or smokeless tobacco[15] components, or they can derive from in vivo reduction of nitroaromatic precursors.[16−18] In particular, it is generally assumed that aromatic amines are enzymatically oxidized to hydroxylamines, which are in turn enzymatically converted to hydroxylamine O-sulfate (or O-acetate) esters. The heterolytic scission of the N−O bond of the latter species is thought to generate a transient arylnitrenium ion, which reacts with DNA, predominantly at C8 of a guanine residue, to give C8 adducts which cause severe mutations that ultimately lead to cancer tumors.[19]

Although guanosine is the major site of reaction with arylnitrenium ion in vitro and in vivo, it is known that other purines and pyrimidines react with arylnitrenium ion to form minor adducts.[20] In particular, it has been reported that adenosine also forms a C8 adduct.[20] For example, Beland and co-workers studied the reaction of 4-aminobiphenyl nitrenium ion with DNA at pH 5, and a C8 adduct of adenosine (Scheme 1) was obtained.[21] However, in a experiment by Kennedy et al., the reactions of arylnitrenium ions with adenosine produced a unique benzene imine N6 adduct (Scheme 1) and no C8 adduct was found.[22] Therefore, it is not clear what kind of adducts could be formed in the reactions of arylnitrenium ions with adenosine, C8 adduct, N6 adduct, or other adducts. On the other hand, the mechanisms of different carcinogen−nucleic acid adducts formed are also poorly understood even for widely researched reactions of arylnitrenium ions with guanosine. For instance, three controversial mechanisms of the reaction between arylnitrenium ion and guanosine or deoxyguanosine (dG) have been proposed in experiments.[22−24]

Theoretical studies on reaction mechanisms involving nitrenium ions and their reduced forms have been performed for a long time.[25−32] Among these explorations, Platz, Gritsan, Bally, and Borden carried out systematic ab initio studies that play important roles in the understanding of arylnitrene rearrangements.[25,26,28−30] Sullivan and Cramer[31] employed quantum chemical calculations to reveal the mechanism for self-destruc-

(7) (a) Novak, M.; Toth, K.; Rajagopal, S.; Brooks, M.; Hott, L. L.; Moslener, M. *J. Am. Chem. Soc.* **2002**, *124*, 7972. (b) Novak, M.; Kazerani, S. *J. Am. Chem. Soc.* **2000**, *122*, 3606. (c) Novak, M.; Kahley, M. J.; Lin, J.; Kennedy, S. A.; Swanegan, L. A. *J. Am. Chem. Soc.* **1994**, *116*, 11626.
(8) (a) Zhu, P.; Ong, S. Y.; Chan, P. Y.; Leung, K. H.; Phillips, D. L. *J. Am. Chem. Soc.* **2001**, *123*, 2645. (b) Ong, S. Y.; Zhu, P.; Poon, Y. F.; Leung, K. H.; Fang, W.-H.; Phillips, D. L. *Chem. Eur. J.* **2002**, *8*, 2163.
(9) Michalak, J.; Zhai, H. B.; Platz, M. S. *J. Phys. Chem.* **1996**, *100*, 14028.
(10) Novak, M.; Kennedy, S. A. *J. Phys. Org. Chem.* **1998**, *11*, 71.
(11) Radomski, J. L.; Brill, E. *Science* **1970**, *167*, 992.
(12) Kadlubar, F. F.; Miller, J. A.; Miller, E. C. *Cancer Res.* **1978**, *36*, 1196.
(13) Thorgairsson, S. S.; Wirth, P. J.; Staiano, N.; Smith, C. L. *Adv. Exp. Med. Biol.* **1982**, *136B*, 897.
(14) Knize, M. G.; Cunningham, P. L.; Griffin, E. A.; Jones, A. L.; Felton, J. S. *Food Chem. Toxicol.* **1994**, *32*, 15.
(15) Stamm, S. C.; Zhong, B.-Z.; Zhong, W.-Z.; Ong, T. *Mutat. Res.* **1994**, *321*, 253.
(16) Herreno-Saenz, D.; Evans, F. E.; Abian, J.; Fu, P. P. *Carcinogenesis* **1993**, *14*, 1065.
(17) Herreno-Saenz, D.; Evans, F. E.; Fu, P. P. *Chem. Res. Toxicol.* **1994**, *7*, 806.
(18) Herreno-Saenz, D.; Evans, F. E.; Beland, F. A.; Fu, P. P. *Chem. Res. Toxicol.* **1995**, *8*, 269.
(19) (a) Davidse, P. A.; Kahley, M. J.; McClelland, R. A.; Novak, M. *J. Am. Chem. Soc.* **1994**, *116*, 4513. (b) Miller, J. A.; Miller, E. C. *Environ. Health Perspect.* **1983**, *49*, 3.
(20) (a) Beland, F. A.; Kadlubar, F. F. In *Chemical Carcinogenesis and Mutagenesis I*; Cooper, C. S., Grover, P. L., Eds.; Springer-Verlag: Berlin, Germany, 1990; p 267. (b) Swaminathan, S.; Frederickson, S. M.; Hatcher, J. F. *Carcinogenesis* **1994**, *14*, 611. (c) Scribner, J. D.; Smith, P. L.; McCloskey, J. A. *J. Org. Chem.* **1978**, *43*, 2085.
(21) Beland, F. A.; Beranek, D. T.; Dooley, K. L.; Heflich, R. H.; Kandlubar, F. F. *Environ. Health Perspect.* **1983**, *49*, 125.
(22) Kennedy, S. A.; Novak, M.; Kolb, B. A. *J. Am. Chem. Soc.* **1997**, *119*, 7654.
(23) Humphreys, W. G.; Kadlubar, F. F.; Guengerich, F. P. *Proc. Natl. Acad. Sci. U.S.A.* **1992**, *89*, 8278.
(24) McClelland, R. A.; Dicks, A. A.; Licence, V. E. *J. Am. Chem. Soc.* **1999**, *121*, 3303.
(25) Gritsan, N. P.; Platz, M. S. *Chem. Rev.* **2006**, *106*, 3844.
(26) Tsao, M.-L.; Gritsan, N.; James, T. R.; Platz, M. S.; Hrovat, D. A.; Borden, W. T. *J. Am. Chem. Soc.* **2003**, *125*, 9343.
(27) Burdzinski, G.; Hackett, J. C.; Wang, J.; Gustafson, T. L.; Hadad, C. M.; Platz, M. S. *J. Am. Chem. Soc.* **2006**, *128*, 13402.
(28) Maltsev, A.; Bally, T.; Tsao, M.-L.; Platz, M. S.; Kuhn, A.; Vosswinkel, M.; Wentrup, C. *J. Am. Chem. Soc.* **2004**, *126*, 237.
(29) (a) Carra, C.; Nussbaum, R.; Bally, T. *ChemPhysChem* **2006**, *7*, 1268. (b) Pritchina, E. A.; Gritsan, N. P.; Bally, T. *Phys. Chem. Chem. Phys.* **2006**, *8*, 719.
(30) Borden, W. T.; Gritsan, N. P.; Hadad, C. M.; Karney, W. L.; Kemnitz, C. R.; Platz, M. S. *Acc. Chem. Res.* **2000**, *33*, 765.
(31) Sullivan, M. B.; Cramer, C. J. *J. Am. Chem. Soc.* **2000**, *122*, 5588.
(32) Parks, J. M.; Ford, G. P.; Cramer, C. J. *J. Org. Chem.* **2001**, *66*, 8997.

tion of heteroarylnitrenium ions. Parks et al.[32] first investigated the reaction of guanine with the phenylnitrenium ion theoretically, and studied the conversion of N7 adduct to C8 adduct.

To our knowledge, no theoretical work investigates the reactions of arylnitrenium ions with adenosine in detail. On the other hand, for the formation of the unusual imine adduct in these carcinogenic reactions, there are also too many issues, such as what is the detailed mechanism of its formation, why is the C8 adduct not obtained, etc. Satisfactory answers to these questions are desired. Hence, in this paper, we present a density functional theory (DFT) and high-level ab initio study of the formation mechanism of the unusual benzene imine N6 adduct in the model reaction of 4-biphenylylnitrenium ion with adenine.

2. Theoretical Methods

The following ab initio and DFT calculations were performed using the GAUSSIAN 03 suite of programs[33]on the SGI-3700 Server with 64 CPUs.

The test calculations have been performed (detailed data can be found in Tables S2 and S3, Supporting Information). Finally, all structures of reactants, transition states (TS), intermediates, and products in the reaction of adenine with 4-biphenylylnitrenium ion (only one of its two conformers was considered in the paper because the reactions of two conformers of 4-biphenylylnitrenium ion with adenine are similar) were optimized at the B3LYP[34]/6-31+G(d,p) and B3PW91[35]/6-31+G(d,p) levels of theory. All stationary points were characterized as minima or transition states by vibration frequency calculations at the same level of theory as the geometry optimizations had been done. In addition, all transition states have been analyzed either by calculating an intrinsic reaction coordinate (IRC)[36,37] or by visual inspection of the transition vector with the correct vibration.[38] Frequency calculations at 298 K and 101.325 kPa using the same level of geometries optimized gave the zero-point, thermal, and Gibbs free energy corrections.

The solvent phase calculations were completed at the optimized geometries of gas phase, using the self-consistent reaction field (SCRF)[39,40] method. Tomasi found that the free energy of solvation could be accurately computed using the optimized geometry in vacuo at the same level of theory.[41] In addition, utilizing the geometries obtained at B3LYP/6-31+G(d,p) and B3PW91/6-31+G(d,p) levels in the gas phase, the single-point energies were respectively performed at B3LYP/6-311++G(3df,3pd) and B3PW91/6-311++G(3df,3pd) levels in aqueous solution. The relative stabilities of several TSs are very important in obtaining a correct reaction mechanism of the imine adduct formation. Therefore, their single-point energies were recalculated at some DFT computational levels. First, previous theoretical studies[42] of arylnitrenium ions have demonstrated that the BPW91/cc-pVDZ[43] method could predict accurate energies of state splittings. Thus, the relative stabilities of the several important TSs were evaluated at this level employing the geometries optimized at B3LYP/6-31+G(d,p) and B3PW91/6-31+G(d,p) levels of theory. Second, it has been shown empirically that the BH&HLYP method gives more accurate barrier heights than B3LYP.[44] Thus, relative stabilities of the several important TSs were recalculated at the BH&HLYP[45]/6-311++G(3df,3pd) level on the basis of geometries optimized at B3LYP/6-31+G(d,p) and B3PW91/6-31+G(d,p) levels of theory. In addition, utilizing the geometries optimized at B3LYP/6-31+G(d,p) and B3PW91/6-31+G(d,p) levels of theory, the relative stabilities of the several important TSs were reevaluated at the MP2[46]/6-31+G(d,p) level. High-level MP2/6-311+G(2d,p) and QCISD[47]/cc-pVDZ single-point calculations were also used to examine the relative stabilities of the several important TSs on the basis of optimized geometries at B3LYP/6-31+G(d,p) and B3PW91/6-31+G(d,p) levels of theory. All of the above solution-phase calculations were completed with the IEF-PCM[48] model in GAUSSIAN 03 with use of UAHF atomic radii.

The magnetic shieldings[49] of different imine systems including imine adduct, imine with two water molecules in the model reactions of 4-biphenylylnitrenium ion with adenine and N9-methanol substituted adenine were calculated at the HF/6-31G(d) level on the optimized structures in the gas phase at the B3LYP/6-31G-(d,p) level of theory. The geometries optimized at the B3LYP/6-31+G(d,p) level were used to estimate the effect of the optimization method on NMR chemical shifts of imine adduct. The B3LYP/6-311+G(2d,p) method was also employed to calculate NMR chemical shifts of imine adduct in the reaction of adenine with 4-biphenylylnitrenium ion. On the basis of structures optimized at the B3LYP/6-31G(d,p) level of theory, NMR chemical shifts of imine adduct in the actual reaction of *N*-acetyl-4-aminobiphenyl nitrenium ion with adenosine were obtained at HF/6-31G(d) and B3LYP/6-311+G(2d,p) levels of theory. The default Gauge-Independent Atomic Orbital (GIAO) method as implemented in the Gaussian 03 program was used. NMR chemical shifts were presented relative to tetramethylsilance (TMS).

3. Results and Discussion

3.1. The Results from Density Functional Theory (DFT). 3.1.1. The Initial Attack of Adenine at the Ortho C Site of 4-Biphenylylnitrenium Ion. At the B3PW91/6-31+G(d,p) computational level (the following discussions are all at this level), the schematic aqueous Gibbs free energy surface from an initial attack of adenine at the ortho C (C14 in Scheme 1)

(33) Frisch, M. J.; Trucks, G. W.; Schlegel, H. B.; Scuseria, G. E.; Robb, M. A.; Cheeseman, J. R.; Montgomery, J. A.; Vreven, T., Jr.; Kudin, K. N.; Burant, J. C.; Millam, J. M.; Iyengar, S. S.; Tomasi, J.; Barone, V.; Mennucci, B.; Cossi, M.; Scalmani, G.; Rega, N.; Petersson, G. A.; Nakatsuji, H.; Hada, M.; Ehara, M.; Toyota, K.; Fukuda, R.; Hasegawa, J.; Ishida, M.; Nakajima, T.; Honda, Y.; Kitao, O.; Nakai, H.; Klene, M.; Li, X.; Knox, J. E.; Hratchian, H. P.; Cross, J. B.; Bakken, V.; Adamo, C.; Jaramillo, J.; Gomperts, R.; Stratmann, R. E.; Yazyev, O.; Austin, A. J.; Cammi, R.; Pomelli, C.; Ochterski, J. W.; Ayala, P. Y.; Morokuma, K.; Voth, G. A.; Salvador, P.; Dannenberg, J. J.; Zakrzewski, V. G.; Dapprich, S.; Daniels, A. D.; Strain, M. C.; Farkas, O.; Malick, D. K.; Rabuck, A. D.; Raghavachari, K.; Foresman, J. B.; Ortiz, J. V.; Cui, Q.; Baboul, A. G.; Clifford, S.; Cioslowski, J.; Stefanov, B. B.; Liu, G.; Liashenko, A.; Piskorz, P.; Komaromi, I.; Martin, R. L.; Fox, D. J.; Keith, T.; Al-Laham, M. A.; Peng, C. Y.; Nanayakkara, A.; Challacombe, M.; Gill, P. M. W.; Johnson, B.; Chen, W.; Wong, M. W.; Gonzalez, C.; Pople, J. A. *Gaussian 03*, Revision D.01; Gaussian, Inc.: Wallingford, CT, 2004.

(34) (a) Becke, A. D. *J. Chem. Phys.* **1993**, *98*, 5648. (b) Lee, W.; Yang, W.; Parr, R. G. *Phys. Rev. B* **1988**, *37*, 785.

(35) Perdew, J. P.; Wang, Y. *Phys. Rev. B* **1992**, *45*, 13244.

(36) Gonzalez, C.; Schlegel, H. B. *J. Chem. Phys.* **1989**, *90*, 2154.

(37) Gonzalez, C.; Schlegel, H. B. *J. Phys. Chem. A* **1990**, *94*, 5523.

(38) Frisch, A. E.; Dennington, R. D.; Keith, T. A.; Nielsen, A. B.; Holder, A. J. *GaussView*, Rev. 3.07; Gaussian Inc.: Pittsburgh, PA, 2003.

(39) Cammi, R.; Mennucci, B.; Tomasi, J. *J. Phys. Chem. A* **2000**, *104*, 5631.

(40) Cammi, R.; Mennucci, B.; Tomasi, J. *J. Phys. Chem. A* **1999**, *103*, 9100.

(41) Barone, V.; Cossi. M.; Mennucci, B.; Tomasi, J. *J. Chem. Phys.* **1997**, *107*, 3210.

(42) (a) Schreiner, P. R.; Karney, W. L.; Schleyer, P. v. R.; Borden, W. T.; Hamilton, T. P.; Schaefer, H. F., III *J. Org. Chem.* **1996**, *61*, 7030. (b) Patterson, E. V.; McMahon, R. J. *J. Org. Chem.* **1997**, *62*, 4398. (c) Sulzbach, H. M.; Platz, M. S.; Schaefer, H. F., III; Haddad, C. M. *J. Am. Chem. Soc.* **1997**, *119*, 5682.

(43) Woon, D. E.; Dunning, T. H., Jr. *J. Chem. Phys.* **1993**, *98*, 1358.

(44) Frisch, A.; Frisch, M. J. *Gaussian 98 Users Reference*; Gaussian Inc.: Pittsburgh, PA, 1998; p 75.

(45) Becke, A. D. *J. Chem. Phys.* **1993**, *98*, 1372.

(46) Moller, C.; Plesset, M. *Phys. Rev.* **1934**, *46*, 618.

(47) Pople, J. A.; Head-Gordon, M.; Raghavachari, K. J. *J. Chem. Phys.* **1987**, *87*, 5968.

(48) Tomasi, J.; Mennucci, B.; Cances, E. *J. Mol. Struct.* (*THEOCHEM*) **1999**, *464*, 211.

(49) Gauss, J. *J. Chem. Phys.* **1993**, *99*, 3629.

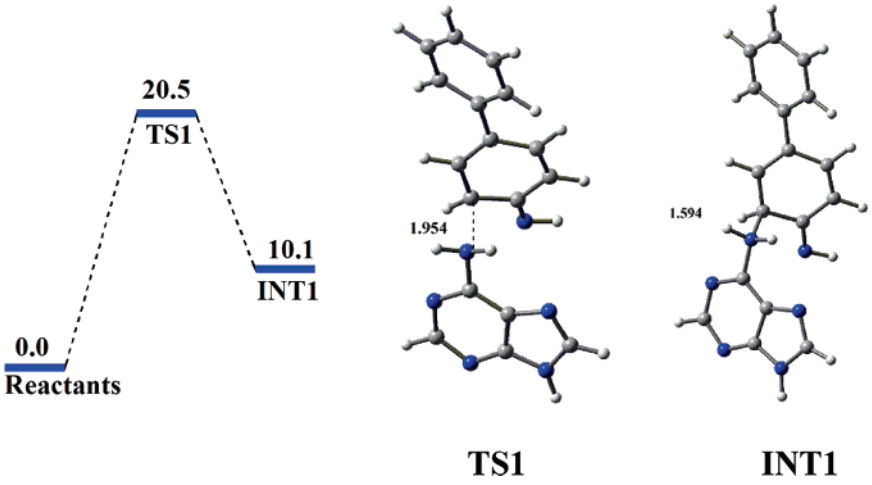

FIGURE 1. The schematic aqueous Gibbs free energy surface and structures of stable points from an initial attack of adenine at the ortho C site of 4-biphenylylnitrenium ion at the B3PW91/6-31+G(d,p) level of theory.

site of 4-biphenylylnitrenium ion is plotted in Figure 1. This attack proceeds through a transition state TS1 to form an intermediate INT1 that is 10.1 kcal/mol higher in energy than the separated reactants. As presented in Figure 1, the N6′-C14 distances of TS1 and INT1 are respectively 1.954 and 1.594 Å. Some alternative conformers of TS1 in the initial ortho attacks are given in Figure S1 of the Supporting Information. We discuss here only TS1 because it is the lowest in energy in the MP2/6-311+G(2d,p)/IEFPCM//B3PW91/6-31+G(d,p)+ZPE calculations in these ortho attacks. In fact, in another initial ortho attack (see Figure S2 in the Supporting Information), there are three possible pathways to imine adduct and azepine adduct. But thermodynamics precludes their formation (detailed discussions are presented in the Supporting Information). Therefore the most probable product in this ortho attack is INT1.

3.1.2. The Initial Attack of Adenine at the Para C Site of 4-Biphenylylnitrenium Ion. Now we examine an additional reaction pathway. A more likely mechanism is the initial attack of adenine N6 on the para C site of arylnitrenium ion (C10 site in Scheme 1) because the site is the preferred site of attack of several nucleophiles, including water. In the following, we will discuss this attack at the B3PW91/6-31+G(d,p) computational level.

The schematic aqueous Gibbs free energy surface from an initial attack of adenine at the para (C10 in Scheme 1) site of 4-biphenylylnitrenium ion is plotted in Figure 2. In this attack, the reactants first form an ion−molecule complex COM21, and it goes across a transition state TS21 in Figure 3 to form an intermediate INT21, which simultaneously proceeds to N6′ deprotonated and N13′ protonated processes to become intermediate INT22 (we name it the N6′ protonated imine adduct). The N6′ protonated imine adduct can convert to imine adduct by the N6′ deprotonation step. Compared with this para attack, the energetics of the ortho attack is more favorable at the B3PW91/6-31+G(d,p) level of theory. As shown in Figures 1 and 2, the transition state TS21 (25.6 kcal/mol) lies higher in energy than the TS1 (20.5 kcal/mol). Hence, at the B3PW91/6-31+G(d,p) level of theory, the ortho attack should be the more feasible. In other words, the intermediate INT1 is a more probable product than imine or azepine adducts. Some alternative conformers of TS21 in the initial para attacks are given in Figure S1 of the Supporting Information. We discuss here only TS21 because it is the lowest in energy in the MP2/6-311+G-

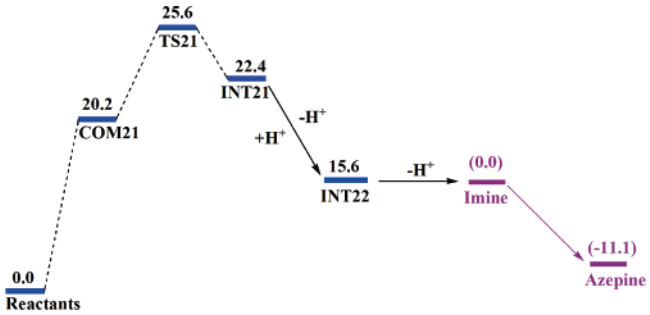

FIGURE 2. The schematic aqueous Gibbs free energy surface of N6 imine adduct formed by the initial attack of adenine at the para C (C10 in Scheme 1) site of 4-biphenylylnitrenium ion at the B3PW91/6-31+G(d,p) level of theory. The energy of the azepine adduct is relative to that of the imine adduct.

(2d,p)/IEFPCM//B3PW91/6-31+G(d,p)+ZPE calculations in these para and ortho attacks.

3.1.3. Different DFT Methods for Examining the Ortho and Para Attacks. In the preceding sections, we have examined two kinds of attacks in the reaction of adenine with 4-biphenylylnitrenium ion at the B3PW91/6-31+G(d,p) level of theory. But no imine or azepine adducts can be obtained, only an intermediate INT1 is the most probable product at this level of theory. Thus, it is necessary to evaluate the energetics of the two kinds of attacks by using various DFT methods. The relative stability of TS1 and TS21 is very important for drawing a conclusion of which attack is more feasible. Hence, in this section, we proceed with evaluating the relative stabilities of these transition states using some DFT computational methods. The obtained energies and Gibbs free energies of TS1 and TS21 relative to the separated reactants are collected in Table 1.

First, two DFT methods via B3LYP and B3PW91 with different basis sets were employed to evaluate the energetics of these TSs. From the data in Table 1, we can find that the aqueous energy and Gibbs free energy of TS1 in the ortho attack is still lower than those of TS21 in the para attack. Thus, the ortho attack is still more feasible than the para attack when B3LYP and B3PW91 methods are employed.

Then we employed the BPW91/cc-pVDZ method to obtain the energies and Gibbs free energies of TS1 and TS21 relative to the separated reactants both in the gas phase and in aqueous

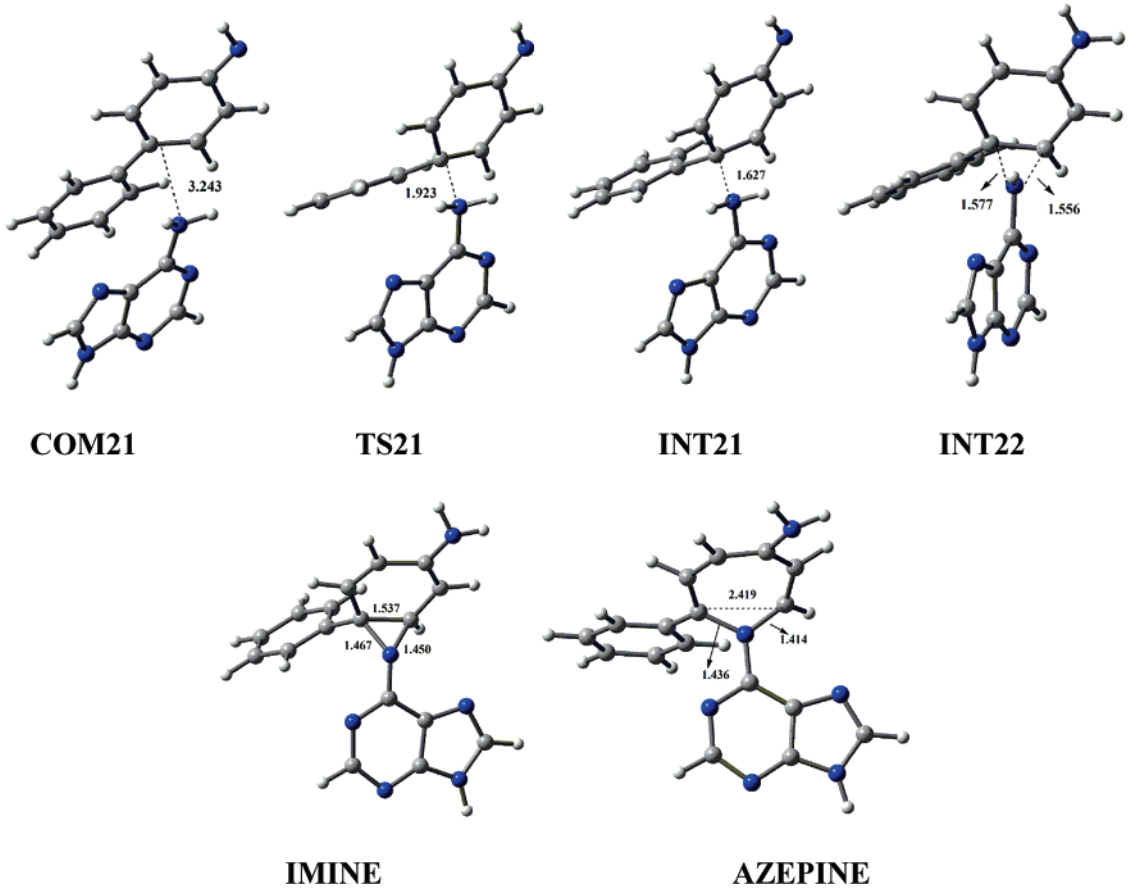

FIGURE 3. The B3PW91/6-31+G(d,p) optimized geometries of ion−molecule complex (COM), transition states (TS), intermediate (INT), imine, and azepine adducts in the initial attack of adenine at the para C site of 4-biphenylylnitrenium ion.

TABLE 1. The Relative Energies (Gibbs Free Energies) Relative to the Separated Reactants of TS1 and TS21 in the Ortho and Para Attacks at Several Levels of Density Functional Theory

	gas phase		aqueous soln	
methods	TS1	TS21	TS1	TS21
B3LYP/6−31+G(d,p)//A[a]	0.8 (15.0)	6.3 (21.0)	6.8 (24.0)	11.0 (29.5)
B3PW91/6−31+G(d,p)//B[b]	−1.5 (11.4)	3.4 (16.5)	4.7 (20.5)	8.8 (25.6)
B3LYP/6−311++G(3df,3pd)//A[a]	2.0 (16.2)	7.4 (22.1)	7.6 (21.8)	11.8 (26.5)
B3PW91/6−311++G(3df,3pd)//B[b]	−0.4 (12.4)	4.1 (17.2)	5.4 (18.2)	9.3 (22.3)
BPW91/cc−pVDZ//A[a]	−4.0 (10.2)	2.1 (16.8)	1.8 (16.0)	6.7 (21.4)
BPW91/cc−pVDZ//B[b]	−4.5 (8.4)	1.4 (14.5)	1.4 (14.3)	6.5 (19.5)
BH&HLYP/6−311++G(3df,3pd)//A[a]	1.8 (16.1)	4.5 (19.2)	7.4 (21.7)	9.2 (23.9)
BH&HLYP/6−311++G(3df,3pd)//B[b]	2.1 (14.9)	4.8 (17.9)	7.8 (20.6)	10.1 (23.2)

[a] A denotes geometries optimized at the B3LYP/6-31+G(d,p) level of theory. [b] B denotes geometries optimized at the B3PW91/6-31+G(d,p) level of theory.

solution on the basis of geometries optimized at B3LYP/6-31+G(d,p) and B3PW91/6-31+G(d,p) levels of theory, because previous studies have demonstrated that the BPW91/cc-pVDZ method can predict state splittings of nitrenium ions within about 2 kcal/mol as compared to either experimental or better-converged quantum mechanical calculations.[44] As listed in Table 1, the results from all BPW91/cc-pVDZ calculations indicate that the aqueous energy and free energy of TS1 are still lower than those of TS21. Therefore, BPW91/cc-pVDZ calculations also support the conclusion that the ortho attack is still more feasible than the para attack.

It has been shown empirically that the BH&HLYP method gives more accurate barrier heights than the B3LYP method. The reason for this is that the BH&HLYP method most significantly differs from B3LYP in that the HF exchange is set to 50%, but this significantly decreases the accuracy of calculated bond energies and energies of reaction at the same time and only improves calculated barrier heights.[50] For a further investigation, on the basis of TS1 and TS21 geometries optimized at B3LYP/6-31+G(d,p) and B3PW91/6-31+G(d,p) levels of theory, their single-point energies have been evaluated at the BH&HLYP/6-311++G(3df,3pd) level of theory. These results are also provided in Table 1. We can see that the energy and free energy of TS1 are generally lower than those of TS21 both in the gas phase and in the aqueous solution. Compared with the results from BPW91/cc-pVDZ calculations, the energy and free energy of TS1 are closer to those of TS21, particularly in aqueous solution. Hence, the results from BH&HLYP methods still favor the conclusion that the ortho attack is more feasible than the para attack.

3.2. Reevaluation the Energetics of TS1 and TS21 by Using High-Level ab Initio Methods. All DFT methods used in the above sections reveal that the energy and free energy of TS1 in the ortho attack are lower than those of TS21 in the para attack both in the gas phase and in aqueous solution in the

(50) Lynch, B. J.; Fast, P. L.; Harris, M.; Truhlar, D. G. *J. Phys. Chem. A* **2000**, *104*, 21.

TABLE 2. The Relative Energies (Gibbs Free Energies) of TS1 and TS21 Relative to the Separated Reactants in the Ortho and Para Attacks Evaluated by Using Several High-Level ab Initio Methods

	gas phase		aq soln	
methods	TS1	TS21	TS1	TS21
MP2/6-31+G(d,p)//A[a]	−15.6	−18.8	−10.1	−14.2
	(−1.4)	(−4.1)	(4.2)	(0.6)
MP2/6-31+G(d,p)//B[b]	−15.2	−18.6	−9.4	−13.4
	(−2.3)	(−5.2)	(3.4)	(0.0)
MP2/6-311+G(2d,p)//A[a]	−14.2	−17.0	−8.9	−12.5
	(0.0)	(−2.3)	(5.3)	(2.3)
MP2/6-311+G(2d,p)//B[b]	−13.8	−16.4	−8.3	−11.3
	(−0.9)	(−3.3)	(4.4)	(1.8)
QCISD/cc-pVDZ//B[b]	−11.5	−13.3	−4.8	−8.1
	(4.1)	(−0.3)	(9.5)	(4.9)

[a] A denotes geometries optimized at the B3LYP/6-31+G(d,p) level of theory. [b] B denotes geometries optimized at the B3PW91/6-31+G(d,p) level of theory.

model reaction of adenine with 4-biphenylylnitrenium ion, and the aqueous activation energy of rate-determining TS1 is in the range of 14−24 kcal/mol. In the Kennedy et al. experiment, they observed that the rate constant for the formation of imine adduct is rate limiting, about 3.1×10^7 M^{-1} s^{-1}. Thus, it is concluded that the aqueous activation energy of the rate-determining transition state should be about 7 kcal/mol. It seems that DFT methods could not obtain the accurate activation energy for the studied reaction of arylnitrenium ion with adenine. Therefore, in this section, high-level ab initio calculations are used to reevaluate the energetics of the transition states in the model reaction of adenine with 4-biphenylylnitrenium ion.

First, on the basis of geometries optimized at B3LYP/6-31+G(d,p) and B3PW91/6-31+G(d,p) levels of theory, the energetics of TS1 and TS21 were reevaluated at the MP2/6-31+G(d,p) level of theory. As can be seen from Table 2, the relative stabilities between ortho attack (TS1) and para attack (TS21) from the MP2 calculations are contrary to those from the DFT calculations. For example, with the MP2/6-31+G(d,p)//B3LYP/6-31+G(d,p) method, the aqueous activation energy of TS21 is lower by 3.6 kcal/mol than that of TS1, whereas all used DFT methods provide that the gas and aqueous Gibbs free energies of TS21 are higher than those of TS1. Hence, MP2/6-31+G(d,p) methods support the conclusion that the para attacks are a more feasible pathway to imine adduct than the ortho attacks.

To confirm the above results from the MP2 methods, higher level ab initio calculations were used to estimate the relative stabilities of TS1 and TS21. As we can see from Table 2, using the geometries optimized at B3LYP/6-31+G(d,p) and B3PW91/6-31+G(d,p) levels of theory, the relative stabilities of the five important TSs from MP2/6-311+G(2d,p) single-point calculations are in agreement with those from MP2/6-31+G(d,p) methods, that is, the MP2 methods all reveal that the gas and aqueous Gibbs free energies of TS21 in the para attack are lower than those of TS1 in the ortho attack. It is noted that the energy and Gibbs free energy (relative to the separated reactants) of the transition state TS21 in both gas and aqueous phases estimated by using the MP2 method with larger basis sets (6-311+G(2d,p)) will become higher than those from the MP2 method with modest size basis sets (6-31+G(d,p)). This indicates that the aqueous Gibbs free energies of TSs in the studied reaction may become higher when larger basis sets are used.

The higher level QCISD/cc-pVDZ method was further used to evaluate the relative stabilities of TS1 and TS21 due to contrary conclusions drawn from DFT and MP2 methods. After a large amount of computational effort, the results from the QCISD method were ultimately obtained. As listed in Table 2, the energy and Gibbs free energy (relative to the separated reactants) of TS1 in both gas and aqueous phases from the QCISD/cc-pVDZ calculations become higher than those from MP2/6-311+G(2d,p) calculations. This indicates that the aqueous Gibbs free energies of TSs in the studied reaction may become higher when higher correlation methods are used.

On the basis of MP2 and QCISD results, it is concluded that the aqueous Gibbs free energies of TSs in the studied reaction may be closer to experimental estimation when higher correlation methods with larger basis sets are used. Hence, the conclusion from high-level MP2 and QCISD methods should be ultimately supported, that is, the reaction pathway initiated by attack of adenine at the para C site of 4-biphenylylnitrenium ion is more feasible to the formation of imine adduct than the reaction pathway initiated by attack of adenine at the ortho C site of 4-biphenylylnitrenium ion.

According to above estimations on the relative stability of TS1 and TS21, it can be found that the results from DFT methods and high-level ab initio methods are largely different. What is the origin of this large difference? In fact, the discussions of large difference between DFT methods and high-level ab initio methods have been an active field recently. For example, Schreiner et al.[51] found that many DFT methods are unreliable for computing hydrocarbon isomer energy differences. But they thought that DFT geometries generally are good. Hence, Schreiner et al. recommended the use of higher level, non-DFT energy single points computed at DFT-optimized structure. Check and Gilbert have also observed that large error exists when the B3LYP method is used to estimate reaction energies.[52] Schreiner et al. thought that the large difference between DFT methods and high-level ab initio methods can systematically be traced back to the neglect of dispersion interactions in DFT, which are key for the energy evaluations of, e.g., alkanes.[51] For the reaction system in this study, the existence of the biphenyl cycle may lead to poor evaluation of the DFT method according to the explanation of Schreiner et al. However, some research indicates that the neglect of dispersion cannot be the only source of the error.[53] Similar discussions about the origin of the large difference between DFT methods and high-level ab initio methods are still continuing.[54]

When two various geometries from B3LYP/6-31+G(d,p) and B3PW91/6-31+G(d,p) methods are used in the studied reaction system, which geometry from the two DFT methods has higher quality? In the study[51] of Schreiner et al., they found that B3LYP had difficulties in describing structures with bicyclic hydrocarbons. This is not the case for B3PW91. It outperforms B3LYP. Some other studies also found that the B3LYP method had a large difference from MP2 and higher level ab initio methods.[52−54] In this study, we have tried to optimized the geometry of TS21 using the MP2/cc-pVDZ method. It is found that the TS geometry from the B3PW91 method is closer to that from the MP2 method than the B3LYP method. Detailed data are given

(51) Schreiner, P. R.; Fokin, A. A.; Pascal, R. A.; de Meijere, A. *Org. Lett.* **2006**, *8*, 3635.
(52) Check, C. E.; Gilbert, T. M. *J. Org. Chem.* **2005**, *70*, 9828.
(53) Grimme, S. *Angew. Chem., Int. Ed.* **2006**, *45*, 4460.
(54) Wodrich, M. D.; Corminboeuf, C.; Schleyer, P. v. R. *Org. Lett.* **2006**, *8*, 3631.

TABLE 3. The NMR Chemical Shifts (ppm) of Key Sites for the Different Systems Including Imine Adduct, Azepine Adduct, Imine with Two Water Molecules, N9 Methanol-Substituted Imine Adduct (N9-sub) in the Reactions of 4-Biphenylylnitrenium Ion with Adenine and N9-Methanol-Substituted Adenine along with Theoretical Values and Corresponding Experimental Values (exptl) of These Key Sites in the Actual Imine and Azepine Adducts (actual) Obtained in the Reaction of *N*-Acetyl-4-aminobiphenyl Nitrenium Ion with Adenosine

	azepine system			imine system							
site	azepine	actual	exptl	imine			imine + $2H_2O$		N9-sub	actual	
C5	113.7[a]	115.7[a]	119.6	117.6[a]	117.4[b]	129.6[c]	127.8[c]	116.1[a]	117.6[a]	120.1[a]	132.0[c]
C6	158.3	161.2	150.1	163.9	163.7	164.2	163.0	163.8	157.8	163.6	162.7
C10	127.8	127.3	72.6	44.1	44.2	60.3	61.2	45.2	51.0	42.1	59.1
C11	126.7	123.2	134.1	136.3	136.6	142.5	142.6	136.9	130.5	132.0	137.4
C15	135.3	130.6	62.9	40.4	39.8	53.6	51.9	39.7	46.7	46.2	61.7

[a] IEFPCM-HF/6-31G(d)//B3LYP/6-31G(d,p) method. [b] IEFPCM-HF/6-31G(d)//B3LYP/6-31+G(d,p) method. [c] IEFPCM-B3LYP/6-311+G(2d,p)// B3LYP/6-31G(d,p) method.

in Table S4 in the Supporting Information. But for the geometry of the intermediate in the system studied, B3PW91 and B3LYP methods provide similar results. Hence, on the basis of the above discussions, it is concluded that the results from B3PW91 optimized geometries are more reliable than those from B3LYP.

3.3. The Final Products in the Studied Reaction. In the preceding sections, we have obtained two important reaction pathways for the studied reaction. Density functional theory (DFT) reveals that the reaction pathways initiated by attack of adenine at the ortho C site of 4-biphenylylnitrenium ion are more favorable. However, high-level ab initio calculations including MP2 and QCISD methods support the reaction pathways initiated by attack of adenine at the para C site of 4-biphenylylnitrenium ion are the most feasible pathways to the imine adduct. Considering agreement between aqueous activation energies of transition states in the model reaction from MP2 and QCISD calculations and those estimated from experiment, the conclusion that the reaction pathway of the para attack is the most feasible pathway to the imine adduct should be ultimately supported.

Comparing with the mechanisms of imine adduct formation, is the mechanism of adenine C8 adduct formation feasible? We have explored the mechanism of direct formation of adenine C8 adduct in the same model reaction of adenine with 4-biphenylylnitrenium ion. At the same computation level of B3PW91/6-31+G(d,p), the aqueous activation energy for the transition state related to the direct formation of adenine C8 adduct is 20.7 kcal/mol, whereas the aqueous activation energy for the transition state TS1 is 20.5 kcal/mol. It seems that the formation of adenine C8 adduct is competitive with imine adduct formation when the DFT method is used. However, at the MP2/6-31+G(d,p)//B3PW91/6-31+G(d,p) level of theory, the aqueous activation energy for the transition state related to the direct formation of adenine C8 adduct is 12.6 kcal/mol, whereas the aqueous activation energy for the transition state TS21 is 0.0 kcal/mol. We think that this comparison will become more reasonable when higher level ab initio methods with larger basis sets are used. Thus, the imine adduct should be observed in the studied reactions of arylnitrenium ions with adenosine, and no adenosine C8 adduct can be obtained, which is in fair agreement with the experimental observations.

Can the azepine adduct also be observed in the studied reaction of arylnitrenium ion with adenosine? The results from theoretical calculations on NMR chemical shifts of imine systems indicate that the final product in the studied reaction should not be only imine adduct. Table 3 provides the calculation results on NMR chemical shifts of different imine systems including imine adduct, imine with two water molecules, N9 methanol-substituted imine adduct, and experimental imine adduct. From this, we can see that theoretical NMR chemical shifts of the key sites, particularly C6, C10, and C15 (numbering can be found in Scheme 1), in all researched imine systems are smaller than those from experimental observations, even if the effects of computational methods and the solvent effect on them are considered. According to data listed in Table 3, the NMR chemical shifts of the key sites including C10 and C15 of the azepine system are lager than the experimental values. Therefore, it is concluded that the final products may include azepine adduct. It is noted that Kennedy et al. also provided evidence of dynamic equilibrium between imine adduct and azepine adduct although the NMR chemical shifts showed the final adduct was imine adduct.[22] Since the transition state in the conversion from imine adduct to azepine adduct cannot be located in the present model reaction, a quantitative assessment of imine adduct and azepine adduct in the final products is not provided.

Although the reaction pathway initiated by attack of adenine at the ortho C site of 4-biphenylylnitrenium ion is not the most favorable pathway to the imine adduct, it can provide some inspiration for similar attacks of arylnitrenium ions at the amino group of purines and pyrimidines in this kind of carcinogenic reaction. For instance, the reactions of native DNA with some arylnitrenium ions produced a minor (5−20% compared to C8 adducts) guanosine N2 adduct.[55] It is found that the N2 adduct is more persistent than the C8 adduct in vivo. For this reason, the N2 adduct may be ultimately more important to carcinogenesis than the more abundant C8 adduct.[55] Thus, it is necessary to reveal the formation mechanism of the N2 adduct. The reaction pathways initiated by attack of adenine at the ortho C site of 4-biphenylylnitrenium ion may be used to interpret the formation of the N2 adduct.

Acknowledgment. The authors greatly thank the editor and reviewers for particularly constructive suggestions and comments. This work was supported by the major project (No. 20633050) and grants (Nos. 20403007 and 20373021) from the National Natural Science Foundation of China.

Supporting Information Available: Alternative conformers of TS1 and TS21 (Figure S1) and energetics of these alternative conformers (Table S1), detailed discussions of ortho attack (Figures S2 and(Figure S3), and Cartesian coordinates of the structures for all of the TSs and intermediates. This material is available free of charge via the Internet at http://pubs.acs.org.

JO701980Y

(55) (a) Kriek, E. *Chem.-Biol. Interact.* **1971**, *3*, 19. (b) Meerman, J. H. N.; Beland, F. A.; Mulder, G. J. *Carcinogenesis* **1981**, *2*, 413. (c) Beland, F. A.; Dooley, K. L.; Jackson, C. D. *Cancer Res.* **1982**, *42*, 1348.